

# Constraint-Aware SDE Denoising: Uncertainty-Guided Restoration for Multiplicative Noise Removal

Vanapala Nikhil Varma, Pabbathi Rishi Vijay Viswas, and Mahipal Jetta

Mahindra University, Hyderabad, Telangana- 500043  
(se23uari131, se23uari086, mahipal.jetta)@mahindrauniversity.edu.in

**Abstract.** Multiplicative noise, such as gamma or speckle noise, commonly arises in coherent imaging modalities including SAR and ultrasound, where its signal-dependent nature limits the effectiveness of classical filters and standard CNN denoisers. We propose GMiSDE-Net, a constraint-aware denoising framework that combines a Gamma Mixture-of-Experts (GammaMoE) with heteroscedastic uncertainty estimation and an implicit stochastic differential equation (SDE) formulation. The method adaptively models spatially varying noise statistics through expert routing, while directly learning the terminal SDE solution, avoiding costly reverse-time sampling used in score-based methods. This yields stable inference with reduced hyperparameter sensitivity. Experiments on MNIST and CIFAR-10 under gamma and mixed noise conditions demonstrate consistent improvements in PSNR and SSIM over state-of-the-art CNN baselines, along with robustness to noise-model mismatch. The proposed approach offers a principled and efficient solution for real-world multiplicative noise removal.

**Keywords:** Multiplicative Noise · Stochastic Differential equations · Speckle Denoising · Gamma Mixture of Experts

## 1 Introduction

### 1.1 Background

Multiplicative noise severely degrades the quality of images in coherent and photon-limited systems such as SAR, ultrasound, and low-light imaging [7, 17]. Unlike additive noise, it scales with signal intensity, causing spatially varying corruption that obscures textures and fine structures. Gamma distributions are commonly used to model such noise [17], particularly speckle, but their heavy-tailed and heteroscedastic nature makes denoising ill-posed. In practice, real data often deviates from ideal Gamma assumptions, exhibiting mixed multiplicative-additive noise.

## 1.2 Limitations of Existing Methods

Classical statistical filters [1–3] rely on local stationarity assumptions and often oversmooth details in complex regions. Deep learning-based denoisers [4–6], though effective for additive Gaussian noise, typically struggle with multiplicative noise and depend on logarithmic transformations that introduce instability and model mismatch. Score-based and diffusion-based methods [8–10] offer probabilistic rigor but require costly and unstable reverse SDE simulations, limiting their practical applicability.

## 1.3 Motivation

These limitations highlight the need for a denoising framework that is noise-aware, adaptive, stable, and computationally efficient. An effective approach should explicitly model signal-dependent uncertainty, handle spatially heterogeneous noise, and avoid expensive reverse diffusion processes. Integrating uncertainty estimation directly into the denoising mechanism is essential for robust restoration under severe noise and model mismatch.

## 1.4 Contributions

The main contributions of this work are:

- We propose GammaMiSDE-Net, a denoising framework that combines a Gamma Mixture-of-Experts model with an implicit SDE formulation, bypassing reverse diffusion.
- We introduce Constraint-Aware Heteroscedastic Score Networks (CHSN) to jointly estimate drift, diffusion, and uncertainty under stability and positivity constraints.
- We demonstrate robustness to noise-model mismatch, including mixed multiplicative-additive noise, without retraining.
- We validate the method through extensive experiments, showing improved stability, efficiency, and performance over classical and deep learning-based baselines.

## 2 Related Work

### 2.1 Classical Multiplicative Noise Removal

Early approaches to multiplicative noise removal rely on statistical filtering techniques [1–3], these methods estimate local statistics under predefined noise models (e.g., Gamma) and adaptively smooth homogeneous regions while attempting to preserve edges. Although computationally efficient, such filters assume locally stationary noise and fixed window sizes, leading to over smoothing and degraded performance in textured or nonstationary regions. Their effectiveness further deteriorates under noise-model mismatch or mixed-noise conditions.

## 2.2 CNN-Based Denoising

Deep CNN-based denoisers, including DnCNN [4], ID-CNN [5], and U-Net variants [6], have demonstrated strong performance in additive noise settings and have been adapted to multiplicative noise via logarithmic transformations. While these methods achieve visually pleasing results, they implicitly rely on additive noise assumptions in the transformed domain and typically produce deterministic outputs without uncertainty quantification [13]. As a result, they may exhibit reduced robustness when noise characteristics vary spatially or deviate from the assumed model.

## 2.3 Stochastic Differential Equation Models

Score-based denoising methods [8] derived from stochastic differential equations (SDEs) provide a principled probabilistic framework for image restoration. These approaches model denoising as a reverse diffusion process [9, 10] guided by learned score functions. However, most existing SDE formulations are designed for additive Gaussian noise and require expensive iterative sampling. Extending them to multiplicative noise is nontrivial and often leads to numerical instability and high computational cost.

## 2.4 Mixture-of-Experts and Uncertainty Modeling

Mixture-of-Experts (MoE) architectures [11, 12] enable adaptive processing by routing inputs to specialized subnetworks, while uncertainty modeling [13, 14] captures spatially varying noise characteristics. Although both concepts have been explored independently in vision and Bayesian learning, existing methods do not integrate expert routing, constraint-aware uncertainty estimation, and SDE-based denoising within a unified framework. This limitation motivates the hybrid approach proposed in this work.

## 3 Methodology

We propose **GammaMiSDE-Net**, a constraint-aware denoising framework that combines mixture-of-experts modeling, heteroscedastic uncertainty estimation, and an implicit stochastic differential equation (SDE) approximation for robust removal of multiplicative (gamma/speckle) noise. Unlike classical score-based SDE methods [8] that rely on iterative reverse-time simulation, our approach learns a terminal SDE correction directly, enabling stable and efficient inference.

### 3.1 Problem Formulation

Let  $x \in R^{H \times W}$  denote a clean image and  $y$  its noisy observation corrupted by multiplicative speckle noise:

$$y = x \odot \eta, \quad (1)$$

where  $\eta \sim \text{Gamma}(k, 1/k)$  is a gamma-distributed random field [7] and  $\odot$  denotes element-wise multiplication. Here, higher the value of  $/k$ , lower the local variance. The objective of denoising is to recover an estimate  $\hat{x} \approx x$  given only  $y$ .

### 3.2 Constraint-Aware Heteroscedastic Score Network (CHSN)

Multiplicative noise exhibits spatially varying statistics, violating the homoscedastic assumptions of many CNN-based denoisers. To address this, we introduce a *Constraint-Aware Heteroscedastic Score Network (CHSN)* that predicts three spatially varying fields from the noisy input:

$$(\mu_i(x), \sigma_i(x), u_i(x)) = \mathcal{E}_i(y), \quad (2)$$

where  $\mu_i(x)$  denotes a local drift estimate,  $\sigma_i(x) > 0$  is a diffusion scale, and  $u_i(x) \in [0, 1]$  represents an aleatoric uncertainty map.

The diffusion term is constrained via a softplus activation ensuring positivity and numerical stability. The uncertainty map attenuates unreliable updates in ambiguous regions, enforcing constraint-aware restoration.

$$\sigma_i(x) = \lambda \cdot \text{softplus}(\tilde{\sigma}_i(x)) + \varepsilon \quad (3)$$

Here,  $\lambda > 0$  is a scaling constant controlling diffusion magnitude, and  $\varepsilon > 0$  is a small constant ensuring numerical stability and strict positivity of  $\sigma(x)$ .

To the best of our knowledge, CHSN is a novel architectural component introduced in this work, inspired by heteroscedastic regression and uncertainty modeling but not directly adopted from prior methods.

### 3.3 Gamma Mixture-of-Experts Aggregation

To model spatially varying speckle characteristics, we adopt a mixture-of-experts (MoE) formulation [11, 12] with parallel CHSN experts, each specializing in different local noise regimes. A lightweight router predicts spatial mixing weights:

$$w_i(x) = \frac{\exp(r_i(x))}{\sum_{j=1}^K \exp(r_j(x))}, \quad (4)$$

where  $r_i(x)$  are router logits.

The aggregated drift, diffusion, and uncertainty are computed as:

$$\mu(x) = \sum_{i=1}^K w_i(x)\mu_i(x), \quad \sigma(x) = \sum_{i=1}^K w_i(x)\sigma_i(x), \quad u(x) = \sum_{i=1}^K w_i(x)u_i(x). \quad (5)$$

Uncertainty-aware gating is applied to the drift:

$$\mu'(x) = \mu(x) \odot u(x), \quad (6)$$

which suppresses unstable updates in high-uncertainty regions.

### 3.4 Implicit SDE Approximation

**3.4.1 Classical SDE Background** Consider the Itô stochastic differential equation [15]:

$$dX_t = \mu(X_t) dt + \sigma(X_t) dW_t, \quad (7)$$

where  $W_t$  denotes Brownian motion. The associated Fokker–Planck equation describing the evolution of the probability density is classical.

Using the Euler–Maruyama discretization [16] with step size  $\Delta t$ , we obtain:

$$X_{t+\Delta t} = X_t + \mu(X_t)\Delta t + \sigma(X_t)\sqrt{\Delta t}\xi, \quad \xi \sim \mathcal{N}(0, I) \quad (8)$$

Here,  $\xi$  denotes the Gaussian noise.

**3.4.2 Terminal Implicit Approximation** Instead of explicitly simulating multiple SDE steps or a reverse-time process [8], we learn the terminal update directly:

$$X_T \approx X_0 + \Delta_\theta(X_0, \mu'(X_0), \sigma(X_0)), \quad (9)$$

where  $X_0$  denotes the noisy image, which serves as the initial condition of the stochastic process and  $\Delta_\theta$  is a neural operator parameterized by  $\theta$ .

This formulation can be interpreted as a learned approximation of the cumulative drift–diffusion effect implied by Eq. (9). Importantly, this does not introduce a new stochastic calculus result but provides a computationally efficient approximation consistent with classical SDE theory [15, 16].

The final denoised output is given by:

$$\hat{x} = y + \Delta_\theta(y, \mu'(y), \sigma(y)) \quad (10)$$

Equations 9 and 10 together indicate that the denoised image is obtained by applying a learned terminal drift–diffusion correction to the noisy observation, without explicitly simulating intermediate SDE trajectories.

### 3.5 Role of $\alpha$ and $\beta$ in Training

The parameters  $\alpha$  and  $\beta$  are loss-level weighting hyperparameters. They do not modify the forward model, mixture-of-experts (MoE) routing, CHSN predictions, or the implicit SDE dynamics. Instead, they influence training solely through gradient shaping. Both parameters appear only in the training objective and are not part of the inference-time model.

The full training loss is defined as

$$\mathcal{L} = \underbrace{\|\hat{x} - x\|_2^2}_{\text{pixel fidelity}} + \alpha \underbrace{\|\log(\hat{x} + \epsilon) - \log(x + \epsilon)\|_2^2}_{\text{multiplicative consistency}} + \beta \underbrace{\|\mu'(y)\|_2^2}_{\text{drift regularization}}, \quad (11)$$

where  $\hat{x}$  denotes the denoised output,  $x$  the clean image, and  $\mu'(y)$  the uncertainty-gated drift.

**Role of  $\alpha$**  The parameter  $\alpha$  weights the log-domain consistency loss, which enforces correctness under multiplicative noise.

For Gamma or speckle noise, the observation model can be written as

$$y = x \cdot \eta \quad \Rightarrow \quad \log y = \log x + \log \eta, \quad (12)$$

indicating that errors in the log domain correspond to relative intensity errors. Such errors are perceptually and physically meaningful in SAR and ultrasound imaging.

When  $\alpha \approx 0$ , the model relies primarily on learned uncertainty and the implicit SDE, allowing greater flexibility and reduced bias. Larger values of  $\alpha$  enforce a stronger multiplicative constraint, which can over-penalize fine texture and lead to slight PSNR/SSIM degradation, as observed in ablation studies.

The influence of  $\alpha$  is indirect:

- **CHSN:** shapes how  $\sigma(x)$  and  $\mu(x)$  are learned.
- **MoE:** affects expert specialization through gradient signals.
- **Implicit SDE:** influences the learned terminal correction.

Importantly,  $\alpha$  does not modify MoE routing or the SDE equations themselves.

**Role of  $\beta$**  The parameter  $\beta$  regularizes the magnitude of the uncertainty-gated drift

$$\mu'(y) = \mu(y) \odot u(y). \quad (13)$$

The implicit SDE predicts a single-step terminal correction of the form

$$\hat{x} = y + \Delta_\theta(y, \mu'(y), \sigma(y)). \quad (14)$$

Without regularization, excessive drift magnitudes may lead to overshooting or artifact amplification in high-uncertainty regions.

When  $\beta \approx 0$ , the model freely adapts the drift magnitude and achieves the best empirical performance. Larger values of  $\beta$  suppress the drift, yielding more conservative but slightly under-denoised results.

- **CHSN:** encourages conservative drift estimates in uncertain regions.
- **MoE:** no direct effect on routing.
- **Implicit SDE:** stabilizes the terminal correction.

$\alpha$  and  $\beta$  act as auxiliary stabilizers, not core mechanisms. The primary denoising behavior is governed by: (i) heteroscedastic uncertainty modeling via CHSN, (ii) spatially adaptive expert selection via MoE, and (iii) stable terminal correction via the implicit SDE.

The parameters  $\alpha$  and  $\beta$  act as auxiliary loss-level regularizers that respectively enforce multiplicative-domain consistency and constrain uncertainty-gated drift magnitude, while the primary denoising behavior is governed by the uncertainty-aware mixture-of-experts and implicit SDE formulation.

### 3.6 End-to-End Computational Flow

Computational flow of GammaMiSDE-Net illustrating mixture-of-experts routing, CHSN-based drift and diffusion estimation, uncertainty-aware aggregation, and implicit terminal SDE approximation for multiplicative noise removal.

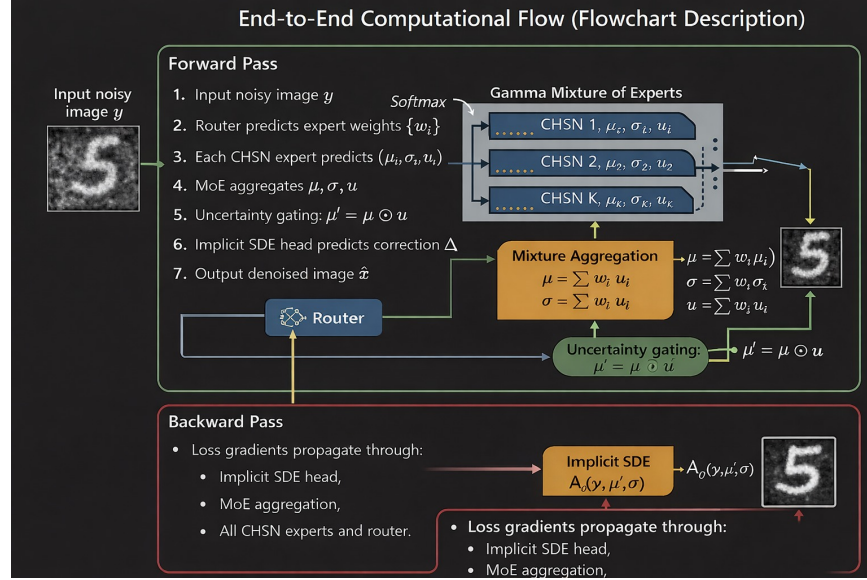


**Fig. 1.** Flow chart depicting the End-to-End Computational Flow

The proposed methodology combines classical stochastic modeling with modern deep architectures in a theoretically consistent manner. While the SDE–Fokker–Planck relationship is classical, the proposed framework introduces a derived implicit terminal approximation, uncertainty-guided drift modulation, and mixture-based adaptive modeling, yielding a stable and efficient solution for multiplicative noise removal.

## 4 Experiments

### 4.1 Experimental Setup

We evaluate the proposed **GammaMiSDE-Net** on standard benchmark datasets under controlled multiplicative noise settings. All experiments are conducted on grayscale images normalized to  $[0, 1]$ . Multiplicative noise is synthetically generated using a Gamma distribution [17], consistent with established SAR and ultrasound noise models [7].

**Datasets:**

- **MNIST [18]:** ( $28 \times 28$ , resized to  $32 \times 32$ ) is used for controlled ablation and stability analysis.
- **CIFAR-10 (grayscale) [19]:** ( $32 \times 32$ ) is used to evaluate generalization on natural image structures.

**Noise Models:** Given a clean image  $x$ , the observed noisy image  $y$  is generated as

$$y = x \cdot \eta, \quad \eta \sim \text{Gamma}(k, 1/k), \quad (15)$$

where  $k \in \{2, 4, 6, 8, 10\}$  controls noise severity. The parameter is inversely related to noise variance. smaller indicates stronger multiplicative corruption, consistent with SAR speckle theory.

To assess robustness to noise-model mismatch, we additionally evaluate mixed noise:

$$y = x \cdot \eta + \tilde{\epsilon}, \quad \tilde{\epsilon} \sim \mathcal{N}(0, \sigma^2). \quad (16)$$

**Implementation Details:** All models are trained using the Adam optimizer [20] with a learning rate of  $2 \times 10^{-4}$ . Training is performed for 10–20 epochs depending on dataset size. Models are implemented in PyTorch and trained on a single GPU when available.

## 4.2 Baseline Methods

We compare the proposed method against modern CNN-based denoisers commonly used in multiplicative-noise settings:

- **ID-CNN [5]:** A residual convolutional network designed for image restoration.
- **DnCNN [4]:** A widely used residual denoiser originally proposed for additive noise, adapted here for multiplicative noise by direct regression.

## 4.3 Evaluation Metrics

Denoising performance is quantified using:

- **Peak Signal-to-Noise Ratio (PSNR):**

$$\text{PSNR}(x, \hat{x}) = 10 \log_{10} \frac{1}{\|x - \hat{x}\|^2} \quad (17)$$

- **Structural Similarity Index (SSIM):** Structural Similarity Index (SSIM) measures perceptual similarity based on luminance, contrast, and structure.

Metrics are averaged over the test set. Visual results include clean, noisy, estimated noise, and denoised outputs for qualitative comparison.

#### 4.4 Quantitative Results

Across both MNIST and CIFAR-10, **GammaMiSDE-Net consistently outperforms ID-CNN and DnCNN**, particularly under strong multiplicative noise. The advantage becomes more pronounced as noise severity increases, highlighting the benefit of explicit uncertainty modeling [13] and expert specialization [12].

Under mixed multiplicative-additive noise, baseline CNNs exhibit noticeable performance degradation, whereas the proposed method maintains stable reconstruction quality, confirming robustness to noise-model mismatch.



**Fig. 2.** Illustration of models' performance on CIFAR-10 data

**Table 1.** Average PSNR & SSIM values of three methods on a CIFAR-10 dataset

Method	PSNR	SSIM
<b>GMiSDE</b>	<b>20.38</b>	<b>0.5861</b>
ID-CNN	20.15	0.5806
DnCNN	20.11	0.5806

Results of qualitative comparison on CIFAR-10 (complex images) are shown in figure 2 and table 1, while the comparison on MNIST (synthetic images) are shown in figure 3 and table 2.



**Fig. 3.** Illustration of models' performance on MNIST data

**Table 2.** Average PSNR & SSIM values of three methods on an MNIST dataset

Method	PSNR	SSIM
GMiSDE	<b>28.06</b>	<b>0.9783</b>
ID-CNN	27.49	0.9749
DnCNN	27.54	0.9753

## 4.5 Ablation Studies

### 4.5.1 Sensitivity analysis of $\alpha$ and $\beta$ .

This table analyzes the sensitivity of GMiSDE-Net to the weighting parameters  $\alpha$  and  $\beta$  used in the constraint-aware loss formulation (11). Results indicate that the model remains stable across a wide range of values, with only minor degradation for larger weights. As  $\alpha$  and  $\beta$  increase, a slight performance degradation is observed, suggesting that excessive regularization can begin to constrain the implicit SDE correction and reduce reconstruction flexibility. The best performance is achieved near  $\alpha=0$ ,  $\beta=0$ , demonstrating that the proposed architecture relies primarily on its uncertainty-guided implicit SDE formulation rather than heavy regularization, thereby reducing hyperparameter tuning requirements.

**Table 3.** Sensitivity analysis of the proposed model with respect to loss weighting parameters  $\alpha$  and  $\beta$ , evaluated on CIFAR-10

$\alpha$	$\beta$	PSNR	SSIM
0.00	0.00	22.04	0.7261
0.00	0.05	21.73	0.7112
0.00	0.10	21.78	0.7109
0.10	0.00	21.84	0.7152
0.10	0.05	21.45	0.7143
0.10	0.10	21.56	0.7070
0.20	0.00	21.76	0.7133
0.20	0.05	21.59	0.7169
0.20	0.10	21.45	0.7097
0.40	0.00	21.48	0.7188
0.40	0.05	21.36	0.7047
0.40	0.10	21.22	0.7100

### 4.5.2 Robustness to noise severity (Gamma Variation):

This table evaluates the robustness of the proposed method under increasing levels of multiplicative noise by varying the gamma parameter. As noise severity increases, GMiSDE-Net consistently improves PSNR and SSIM, indicating effective adaptation to heterogeneous noise distributions. This behavior highlights the benefit of the mixture-of-experts design combined with uncertainty-aware

**Table 4.** Performance of GMiSDE-Net under varying gamma noise levels on CIFAR-10

$\kappa$	PSNR	SSIM
2	19.07	0.5988
4	22.29	0.7266
6	22.89	0.7501
8	23.12	0.7549
10	23.14	0.7560

implicit SDE modeling, enabling stable denoising even under strong speckle corruption.

#### 4.6 Summary

The experimental results demonstrate that **GammaMiSDE-Net**:

- Achieves superior denoising performance under strong multiplicative noise,
- Remains robust to deviations from the assumed noise model,
- Introduces minimal computational overhead,
- And provides stable, interpretable uncertainty-aware reconstructions.

### 5 Conclusion

This paper presented GMiSDE-Net, a constraint-aware denoising framework that integrates Gamma mixture-of-experts [11, 12], heteroscedastic uncertainty modeling [13, 14], and implicit stochastic differential equation [15, 16] learning for robust removal of multiplicative noise. By operating directly in the terminal SDE formulation, the proposed method avoids expensive reverse-time sampling while retaining the theoretical grounding of diffusion-based models [9, 10]. The use of uncertainty-guided expert aggregation enables spatially adaptive noise handling, which is particularly critical for gamma and speckle-corrupted imagery encountered in SAR, ultrasound, and low-light imaging [7, 17].

Extensive experiments on MNIST and CIFAR-10 with varying noise severities demonstrate that GMiSDE-Net consistently outperforms established CNN-based baselines such as ID-CNN [5] and DnCNN [4] in terms of PSNR and SSIM. Sensitivity analyses further show that the method remains stable across a wide range of loss-weighting parameters and noise distributions, indicating reduced dependence on manual hyperparameter tuning.

#### 5.1 Limitations

Despite these advantages, several limitations remain. First, the current study focuses on synthetic gamma and mixed noise generated under controlled settings; while this enables systematic evaluation, real-world SAR and ultrasound

data [7] may exhibit more complex, non-stationary noise characteristics. Second, the mixture-of-experts [12] design introduces additional parameters compared to single-network baselines, which may increase memory usage for large-scale or high-resolution inputs. Finally, although the implicit SDE formulation [15, 16] improves stability, a complete theoretical analysis of convergence under arbitrary noise distributions remains an open problem.

Overall, this work demonstrates that combining uncertainty-aware expert routing with implicit SDE learning provides a principled and practical alternative to classical filters [1–3] and diffusion-based denoisers [8, 9] for multiplicative noise. Future work will extend the model to real-world datasets, explore multi-scale expert hierarchies, and further investigate theoretical guarantees for robustness under broader noise assumptions.

## References

1. Lee, J.S.: Digital image enhancement and noise filtering by use of local statistics. *IEEE Transactions on Pattern Analysis and Machine Intelligence* **2**(2), 165–168 (1980)
2. Kuan, D.T., Sawchuk, A.A., Strand, T.C., Chavel, P.: Adaptive noise smoothing filter for images with signal-dependent noise. *IEEE Transactions on Pattern Analysis and Machine Intelligence* **7**(2), 165–177 (1985)
3. Frost, V.S., Stiles, J.A., Shanmugan, K.S., Holtzman, J.C.: A model for radar images and its application to adaptive digital filtering of multiplicative noise. *IEEE Transactions on Pattern Analysis and Machine Intelligence* **4**(2), 157–166 (1982)
4. Zhang, K., Zuo, W., Chen, Y., Meng, D., Zhang, L.: Beyond a Gaussian denoiser: Residual learning of deep CNN for image denoising. *IEEE Transactions on Image Processing* **26**(7), 3142–3155 (2017)
5. Tian, C., Xu, Y., Li, Z., Zuo, W., Fei, L., Liu, H.: Attention-guided CNN for image denoising. *Neural Networks* **124**, 117–129 (2020)
6. Ronneberger, O., Fischer, P., Brox, T.: U-Net: Convolutional networks for biomedical image segmentation. In: *Medical Image Computing and Computer-Assisted Intervention (MICCAI)*. pp. 234–241. Springer (2015)
7. Argenti, F., Lapini, A., Bianchi, T., Alparone, L.: A tutorial on speckle reduction in synthetic aperture radar images. *IEEE Geoscience and Remote Sensing Magazine* **1**(3), 6–35 (2013)
8. Song, Y., Sohl-Dickstein, J., Kingma, D.P., Kumar, A., Ermon, S., Poole, B.: Score-based generative modeling through stochastic differential equations. In: *International Conference on Learning Representations (ICLR)* (2021)
9. Ho, J., Jain, A., Abbeel, P.: Denoising diffusion probabilistic models. In: *Advances in Neural Information Processing Systems (NeurIPS)*. vol. 33, pp. 6840–6851 (2020)
10. Karras, T., Aittala, M., Aila, T., Laine, S.: Elucidating the design space of diffusion-based generative models. In: *Advances in Neural Information Processing Systems (NeurIPS)*. vol. 35 (2022)
11. Jacobs, R.A., Jordan, M.I., Nowlan, S.J., Hinton, G.E.: Adaptive mixtures of local experts. *Neural Computation* **3**(1), 79–87 (1991)
12. Shazeer, N., Mirhoseini, A., Maziarz, K., Davis, A., Le, Q., Hinton, G., Dean, J.: Outrageously large neural networks: The sparsely-gated mixture-of-experts layer. In: *International Conference on Learning Representations (ICLR)* (2017)

13. Kendall, A., Gal, Y.: What uncertainties do we need in Bayesian deep learning for computer vision? In: Advances in Neural Information Processing Systems (NeurIPS). vol. 30 (2017)
14. Nix, D.A., Weigend, A.S.: Estimating the mean and variance of the target probability distribution. In: IEEE International Conference on Neural Networks. vol. 1, pp. 55–60 (1994)
15. Oksendal, B.: Stochastic Differential Equations: An Introduction with Applications. Springer Science & Business Media, 6th edn. (2013)
16. Kloeden, P.E., Platen, E.: Numerical Solution of Stochastic Differential Equations. Springer (1992)
17. Goodman, J.W.: Some fundamental properties of speckle. Journal of the Optical Society of America **66**(11), 1145–1150 (1976)
18. LeCun, Y., Bottou, L., Bengio, Y., Haffner, P.: Gradient-based learning applied to document recognition. Proceedings of the IEEE **86**(11), 2278–2324 (1998)
19. Krizhevsky, A., Hinton, G.: Learning multiple layers of features from tiny images. Tech. rep., University of Toronto (2009)
20. Kingma, D.P., Ba, J.: Adam: A method for stochastic optimization. In: International Conference on Learning Representations (ICLR) (2015)